doi.org/10.36721/PJPS.2022.35.1.SUP.313-321.1

De novo design of novel spike glycoprotein inhibitors using e-pharmacophore modeling, molecular hybridization, ADMET, quantum mechanics and molecular dynamics studies for COVID-19

Abdulrahim A Alzain[1†], Abdalla Ismail[1†], Mohammed Fadlelmola[1†], Magdi A Mohamed[2†*], Mohanad Mahjoub[1], Alaa A Makki[1] and Tilal Elsaman[2]

[1]Department of Pharmaceutical Chemistry, Faculty of Pharmacy, University of Gezira, Gezira, Sudan
[2]Department of Pharmaceutical Chemistry, College of Pharmacy, Jouf University, Sakaka, Kingdom of Saudi Arabia

Abstract: The pandemic COVID-19, caused by SARS-COV-2, has been a global concern and burden since April 2020 due to high contagiousness and pathogenesis. A great effort is being devoted to identify and investigate different druggable targets for SARS-COV-2 drug discovery. At least three targets have been identified among them is the spike glycoprotein which facilitates viral entry by binding to angiotensin converting enzyme (ACE-2 receptor) in host cell. In the current study, different computational tools were used to design potential cell entry inhibitors targeting spike glycoprotein. The essential pharmacophoric features were identified by e-pharmacophore mapping and fragments virtual screening was run using three different libraries. Docking scores were used to select the best fragments which were linked to afford novel molecules. The designed molecules were filtered via molecular docking, MM-GBSA free energy calculation, ADMET, drug-like properties and DFT calculations. Moreover, synthetic feasibility of the best ligands was studied. These ligands would be envisioned as potential leads for SARS-COV-2 cell entry inhibition and could be explored further towards COVID-19 drug discovery and development.

Keywords: SARS-COV-2, spike glycoprotein, pharmacophore mapping and screening, FBDD, molecular docking, molecular dynamics, DFT

INTRODUCTION

A novel strain of Corona virus, so-called SARS-COV-2, identified at the end of 2019 in Wuhan, China has put the entire world on an alert (Giofre *et al*., 2021). The virus has been recognized to be the causative agent of COVID-19 pandemic (Lai *et al*., 2020) which resulted in nearly 5 million deaths worldwide (Agrawal *et al*., 2021). Since WHO first announcement of COVID-19 as pandemic in March 2020 (Bassi and Hwenda, 2020), extensive literature in COVID-19 has been published covering clinical presentations, diagnosis, pathogenicity, epidemiology, transmission, treatment protocols and vaccines' development (Kaur and Gupta, 2020, Kyriakidis *et al*., 2021, Munir *et al*., 2021, Rahman *et al*., 2021). There are now several COVID-19 vaccines that are in use, nonetheless, their efficacy and long-lasting immunity is questionable specially against newly developed variants (Lopez *et al*., 2021, Tartof *et al*., 2021). Furthermore, unequitable distribution of these vaccines to low-income countries along with vaccine hesitancy and other obstacles have been addressed in the literature (Massinga Loembé and Nkengasong, 2021, Mesa-Vieira *et al*., 2021). Thus, the need for effective drugs has always been mandatory. To this end, a great effort has been devoted to identify and investigate different druggable targets for SARS-COV-2 drug discovery. The viral spike (S) protein has been reported as a potential drug target for COVID-19 drug discovery (Toor *et al*., 2021). The ability of SARS-COV-2 to infect human cells relies primarily on the recognition of the human receptor angiotensin-converting enzyme 2 (ACE2) by the receptor-binding domain (RBD) of S protein promoting viral entry (Ahsan and Sajib, 2021, Ameen *et al*., 2021, Cecon *et al*., 2021, Zhang *et al*., 2021). Spike protein is made up of two subunits, S1 subunit that contains RBD region which is responsible for initial attachment to host receptors and S2 subunit that undergoes several conformational arrangements to form 6-helix bundle (6HB) mediating membrane fusion process (fig. 1) (Gobeil *et al*., 2021, Zeng *et al*., 2021). Thus, targeting SARS-COV-2 S protein is a potential host cell entry inhibitory mechanism that would prevent infection at early stage as a front-line therapeutic target (Sakkiah *et al*., 2020).

Being time consuming, conventional drug discovery might not be the proper approach for COVID-19 drug discovery. Fortunately, in silico drug discovery has become an interesting strategy that cuts short the time needed to come up with a potential lead in terms of activity and drug-like properties (Mohamed *et al*., 2017). Fragment-based drug discovery (FBDD) is a powerful strategy to discover potent small molecule compounds based on fragments that bind weakly to

**Corresponding author:* e-mail: maelhussein@ju.edu.sa

†These authors contributed equally to this work

targets (Li, 2020). The numerous advantages of FBDD over high-throughput drug screening campaigns make it an effective strategy for drug discovery (Choudhury, 2021). With such a strategy, it is easier to screen large number of low molecular weight molecules in a shorter period of time using a variety of biophysical methods (Wilson III *et al*., 2021, Wollenhaupt *et al*., 2020). A wide range of biologically active compounds have been developed using this method. The FDA approved anticancer vemurafenib, for instance, was developed using FBDD (Gupta *et al*., 2021). The current report reveals a new FBDD-based study targeting SARS-COV-2 spike protein for de novo design of viral cell entry inhibitors as promising leads for SARS-COV-2 drug discovery.

MATERIALS AND METHODS

All computation work was conducted using Maestro interface v 12.8 of Schrödinger suite.

Protein retrieval and preparation

The crystallographic structures of SARS-COV-2 S protein with access code (6LZG) and angiotensin-converting enzyme -2 (ACE-2) with access code (1R4L) were downloaded from the PDB database RCSB (http://www.rcsb.org). The crystal 3D structure of each protein was preprocessed by Protein Preparation Wizard incorporated in Maestro. This step is very critical in ensuring that the protein is well prepared for molecular docking studies as it resolves any problem in the protein such as missing atoms, loops or side chains in addition to removal of undesirable elements and rectifying bond orders (Sastry *et al*., 2013). The grids required for ligand docking on RBD were set and boxed up using Glide Receptor Grid Generation tool.

Fragment library preparation

A total of 629774 fragments were retrieved for three libraries namely, Enamine, Asinex and FCH. These fragments were prepared with the aid of Glide LigPrep panel, using default parameters, to minimize the 3D structures, optimize chiralities, produce different protonation sates and generate different conformers (Fadaka *et al*., 2020).

E-pharmacophore model generation and pharmacophore based virtual screening

The amino acid residues at ACE2 binding site of RBD of S protein were selected to build an e-pharmacophore hypothesis using 'Develop a Pharmacophore from Receptor Cavity' option in PHASE application of Schrödinger (Dixon *et al*., 2006). Pharmacophore-based screening was conducted against the Glide generated library, 1184350 fragments, in order to retrieve S protein inhibitors with desired chemical features. Fragments were required to match 4 sites on generated e-pharmacophore hypothesis. Those which matched the set hypothesis were then docked to the S protein using Glide. The docking process was performed in three consecutive steps; first, all fragments were included in high throughput virtual screening (HTVS). Next, SP docking was run for fragments which had docking score ≤ -6.00 kcal/mol. Finally, the top best fragments with SP docking score ≤ -6.00kcal/mol were subjected to XP docking which uses a more sophisticated scoring function that is harder than SP Glide score.

Fragment linking and de novo molecules synthesis

Towards de novo synthesis of novel chemical molecules, the Maestro Breed panel was used for direct linking the top hits fragment, with XP docking score ≤−6.00 kcal/mol, that bound to the active site essential residues in the sub pocket of S protein. The generated new molecules were then prepared using LigPrep for docking process and binding free energy calculations (Fadaka *et al*., 2020).

Molecular docking and binding free energy calculation of the new hybrid compounds

Molecular docking was carried out using Glide application (Friesner *et al*., 2006). The prepared molecules, following Breed de novo hybridization, were run through different levels of docking filters based on the precision of the resultant docking scores against S protein. The top ligands with XP docking score less than −7.00 kcal/mol were also subjected to XP docking against ACE-2 (PDB ID: 1R4L). Candidates with <−7.00 kcal/mol were further processed on Prime module of Schrödinger for Molecular Mechanics-Generalized Born Surface Area (MM-GBSA) to calculate ligands' free binding energies (Jacobson *et al*., 2004).

In silico ADMET prediction

The best ligands, in terms of XP docking scores and MM-GBSA findings, were submitted to Schrödinger Quik Prop module to predict their physicochemical properties, pharmacokinetic profiles and cardiotoxicity. Candidates which revealed satisfactory drug like properties were chosen for molecular dynamic (MD) simulation analyses, density functional theory (DFT) calculations and synthetic accessibility studies (Elbadwi *et al*., 2021).

Density functional theory (DFT) calculation

A couple of molecular and atomic electrostatic characteristics were calculated for the best three compounds (Breeds 1-3) using Jaguar version 12.5 of Schrodinger. The overall quantum-chemical calculations were obtained via the hybrid B3LYP-6-31G** (Becke's three parameters hybrid functional with Lee-Yang-Parr correlation functional LYP at 6-31G** basis set) (Bochevarov *et al*., 2013).

Molecular dynamics (MD) simulation study

Academic Desmond v 6.5, developed by D. E. Shawn Research, was used to run MD studies on the protein-ligand complexes. Solvation was affected in TIP3P water

model box of 10 Å in size. Appropriate counter ions and 0.15 M NaCl were added to neutralize the system which was minimized and heated then thermally relaxed using the system builder default parameters, where force field was set to OPLS3e, simulation time was 50 nanoseconds and temperature (300 K) and pressure (1.01325 bar) were kept constant throughout the process by Nose-Hoover thermostat and Martyna-Tobias-Klein barostat, respectively. During the simulation process, 5208 frames were collected for each system (Bowers *et al*., 2006).

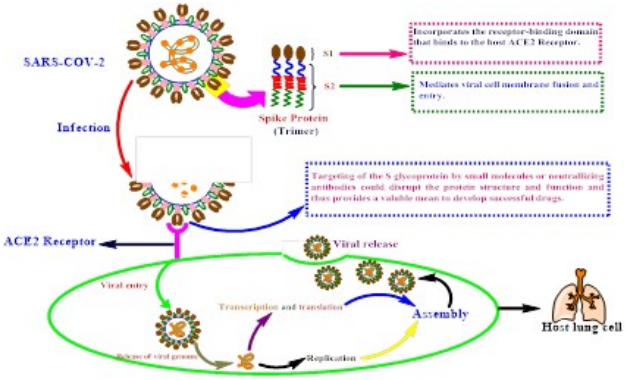

Fig. 1: Role of spike protein in viral cell entry.

Novelty and synthetic accessibility of the best ligands

Zinc Drug-like and ChEMBL (activity <10μM) databases were explored using SwissSimilarity server (Zoete *et al*., 2016) to evaluate novelty of the best ligand Breed 5. In addition, synthetic feasibility was also evaluated in terms of accessibility score (1 to 10) with 1 being very easy and 10 very difficult. Reaction Based Enumeration panel of Schrödinger was used to identify potential retro-synthetic routes for Breed 5 (Konze *et al*., 2019).

RESULTS

Based on the amino acid residues at ACE-RBD interface of S protein, described by Ortega group (Ortega *et al*., 2020), PHASE predicted a seven featured pharmacophore hypothesis (ADDRRN); consisting of one acceptor (A), two donors (D), two aromatic rings (R) and negative charge (N) (fig. 2). Fragments' preparation, using Glide, resulted in a library of 1184350 fragments. Screening of these fragments against four features of the pharmacophore hypothesis revealed 8000 matching fragments. Nearly one eighth of these fragments (110) exhibited docking scores ≤ -6.00 kcal/mol and they were filtered further by SP and XP docking modes in the named order to come up with 81 fragments with XP docking scores ≤ -6.00 kcal/mol. De novo synthesis gave 1848 new ligand hybrids of which 8 ligands (fig. 3) showed promising XP docking scores (≤ -7.00 kcal/mol) with interesting binding interactions at S protein active site. ADMET studies revealed that none of the 8 ligands violated Lipinski rule of five nor showed cardiotoxicity. Furthermore, partition coefficient, aqueous solubility and blood brain permeability parameters were within the accepted limits (table 1). Calculation of binding free energies of ligand-protein complexes of the top 8 breeds using Prime MMGBSA revealed varying outcomes for S complexes compared to ACE-2's (table 1). MD simulation showed that Breed 5 was the most stable among the top 8 ligands as indicated by RMSD values.

DISCUSSION

Four features of the pharmacophore hypothesis were screened against the Glide prepared fragments library (1184350 fragments). Fragments that matched the pharmacophore hypothesis were docked against S protein using Glide HTVS mode.

The process of de novo molecular design involves generation of novel chemical structures that satisfy a desired molecular profile (Meyers *et al*., 2021). The contribution of de novo molecular design strategies in drug discovery is increasing because large chemical spaces could be explored at relatively short time when compared to other computational tools (Walters and Murcko, 2020). Thus, with these top hit fragments in hand, it was now decided to accomplish de novo synthesis of new chemical entities using Breed ligand panel. This resulted in 1848 new ligand hybrids which were submitted to SP docking against S protein. A docking score of ≤ -7.00 kcal/mol was used as a cut-off and thus only 217 ligands were promoted to the next filtering point that was XP docking to reveal 140 ligands with docking scores ≤ -7.00 kcal/mol. A spike glycoprotein / ACE2 dual antagonist could bind to RBD, and compete with the binding of SARS-COV-2 to ACE2 to prevent the virus entry by two mechanisms. Some natural products were reported to possess better spike protein and ACE2 inhibitory activity (Yu and Li, 2021). In the current study, the potential target dual inhibitory activity was assessed. The ligands were docked against ACE-2 protein using XP mode. The study findings revealed that 8 ligands (fig. 3) could act as potential dual inhibitors with a docking scores range of -7.098 to -8.604 kcal/mol, good binding interactions and favorable pharmacokinetics and drug likeness (table 1).

The amino acids in the active site of S protein which interacted with the 8 ligands via hydrogen bonds, as donor or acceptor, were GLN 493, SER 494, GLY 496, ARG 403, GLU 406, TYR 505. Zeng *et al* reported different amino acids involved in the stabilization of the complex formed between S protein and Esculentoside A (Zeng *et al*., 2021). This different binding interaction pattern could be attributed at least to the different chemical nature of interacting ligands. However, similar interaction pattern with most of the aforementioned amino acids residues were observed for some natural products used in Chinese traditional medicine (Yu and Li, 2021). Except for Breed 3, all ligands participated in π-π interactions with TYR

Table 1: Docking scores, MM-GBSA binding free energies and ADMET profiles of the top 8 ligands against S and ACE-2 proteins.

Entry	Spike protein (6LZG)		ACE (1R4L)		Q Plog Po/w[a]	Q Plog S[b]	Q Plog HER[c]	Q Plog BB[d]	Rule of Five[e]
	Docking scores (kcal/mol)	dG_{Bind} (kcal/mol)	Docking scores (kcal/mol)	dG_{Bind} (kcal/mol)					
Breed 1	-8.533	-60.16	-8.235	-57.61	-2.186	-1.479	-3.154	-1.534	0
Breed 2	-8.048	-56.78	-7.849	-44.26	-2.354	-1.611	-3.169	-1.868	0
Breed 3	-7.971	-48.07	-7.846	-37.26	-2.423	-1.376	-2.965	-1.628	0
Breed 4	-8.335	-58.12	-7.788	-48.23	-2.377	-1.38	-3.086	-1.522	0
Breed 5	-7.864	-54.75	-7.638	-37.86	-1.162	-2.428	-3.7	-1.371	0
Breed 6	-8.123	-46.91	-7.466	-24.94	-2.615	-1.402	-2.827	-1.6	0
Breed 7	-7.531	-51.06	-7.358	-23.27	0.644	-2.48	-2.369	-2.553	0
Breed 8	-8.604	-54.63	-7.098	-10.37	-2.983	-1.109	-2.85	-1.963	0

[a]Predicted octanol/water partition coefficient log P (acceptable range -2.0 to 6.5).
[b]Predicted aqueous solubility in mol/L (acceptable range -6.5 to 0.5).
[c]Predicted IC_{50} value for blockage of HERG K+ channels (concern below 5.0).
[d]Predicted blood brain barrier permeability (acceptable range -3 to 1.2).
[e]Lipinski rule of five

Table 2: Quantum chemical properties of best three compounds.

Compounds	HOMO (ev)	LUMO (ev)	HLG (ev)	Solvation energy (kcal/mol)
Breed 3	-0.22373	-0.07358	0.15015	-25.62
Breed 5	-0.23253	-0.07415	0.15833	-23.30
Breed 6	-0.23337	-0.05720	0.17617	-25.62

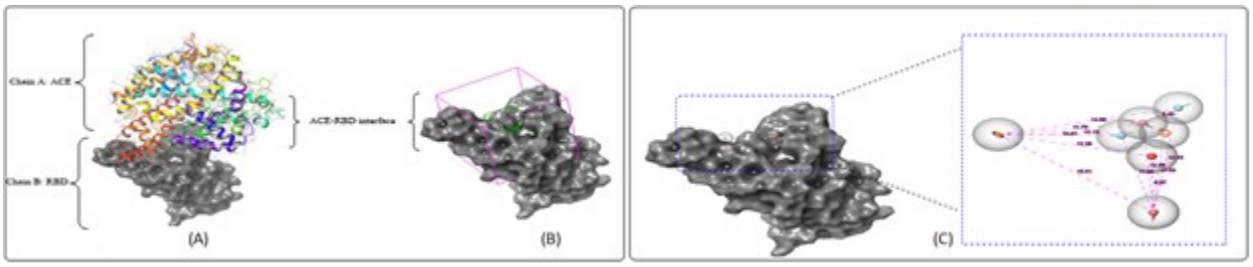

Fig. 2: (A) The two chains of Spike protein (B) Binding site at ACE-RBD interface of S protein (C) Pharmacophore hypothesis at ACE-RBD interface of S protein.

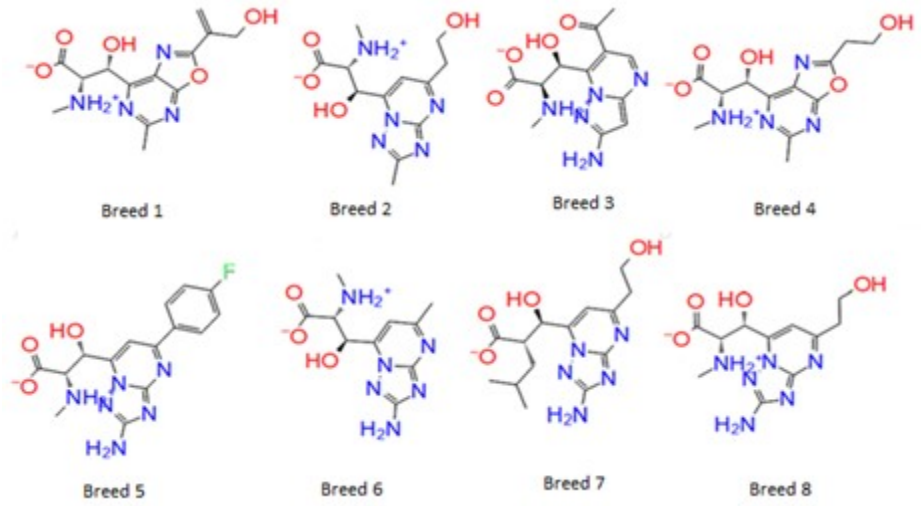

Fig. 3: Top 8 potential SARS-COV-2 entry inhibitors.

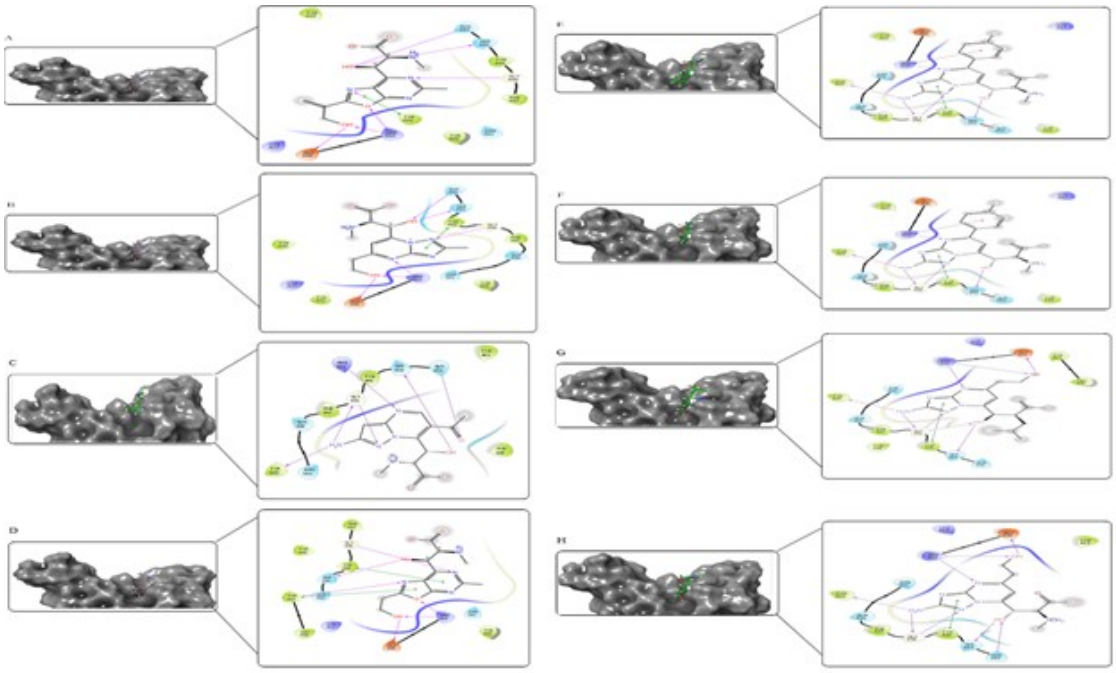

Fig. 4: 2D and 3D interactions of (A) Breed 1 (B) Breed 2 (C) Breed 3 (D) Breed 4 (E) Breed 5 (F) Breed 6 (G) Breed 7 (H) Breed 8 with ACE2-RBD interface of S protein.

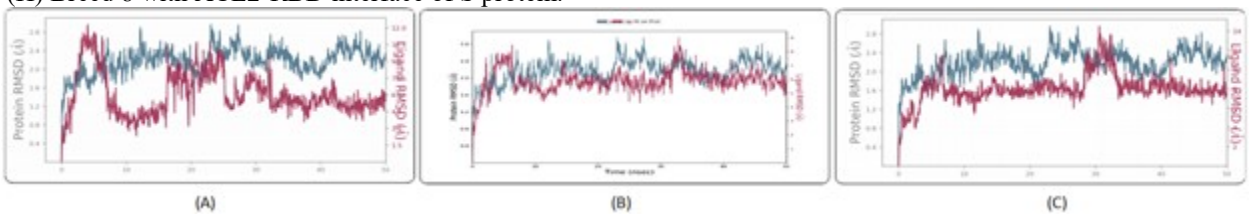

Fig. 5: RMSD plots S protein-ligand interactions of top three stable complexes. (A) Breed 3 (B) Breed 5 (C) Breed 6. The blue color represents backbone protein RMSD. Red color represents ligand RMSD.

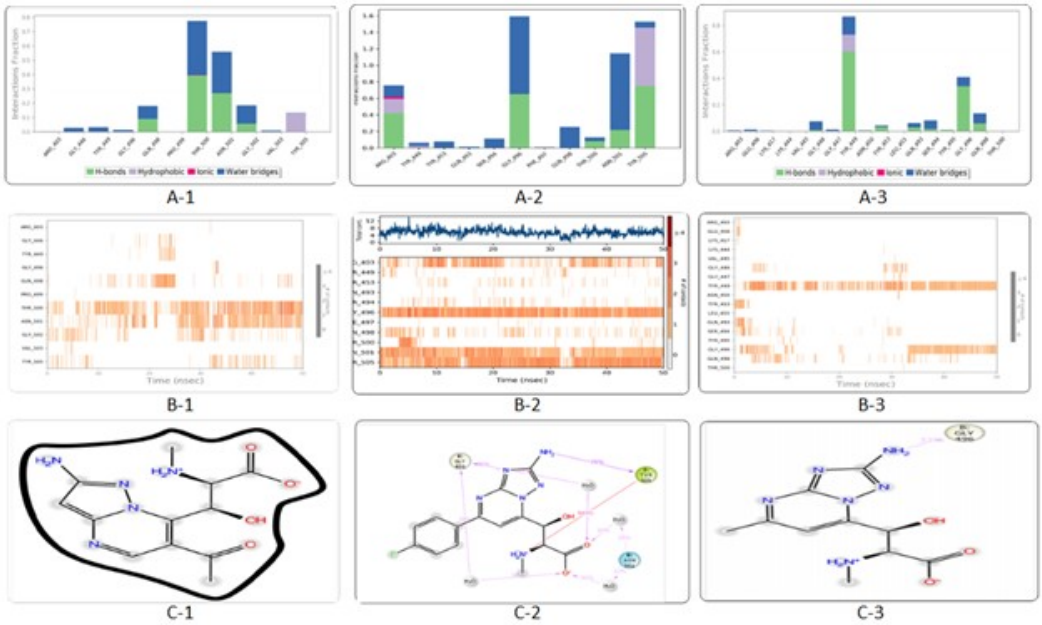

Fig. 6: A1-3: Interactions of Breeds 3, 5 and 6, respectively, with ACE2-RBD interface of S protein; B1-3: Stability of protein ligand contacts for Breeds 3, 5 and 6, respectively (darker color indicates strong contact); C1–3: 2D protein-ligand interactions for Breeds 3, 5 and 6, respectively.

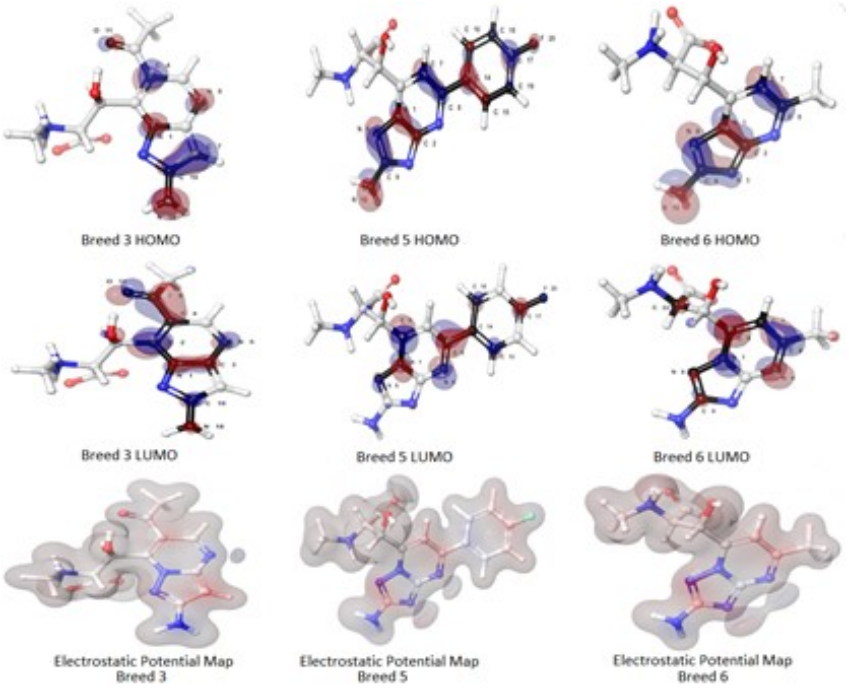

Fig. 7: HOMO-LUMO and electrostatic potential calculations for Breeds 3, 5 and 6.

495, the most, and/or TYR 453. In addition, Breed 5 exhibited π-cation interaction with ARG 403 (fig. 4). Having identified top 8 potential dual cell entry inhibitors, attention was next directed to estimate the interaction strength of each ligand with S and ACE-2 proteins separately. While energies for ACE-2 complexes were inconsistent ranging from -10.37 kcal/mol to -57.61 kcal/mol they were comparable for spike's (-46.91 kcal/mol to -60.16 kcal/mol). It appeared that cell entry inhibitory activity of the new designed molecules would not be mediated through dual inhibition of both S and ACE-2 proteins and it was thus decided to continue the study targeting only S protein.

Conventional docking has a limitation of receptor flexibility and thus resultant protein-ligand complexes' reliability is always questionable. Docking findings can be significantly improved when combined with the expensive, but more accurate molecular dynamic (MD) simulation techniques (Santos *et al*., 2019). MD simulation is a study to assess stability of an investigated ligand when it comes in contact with the active site of its protein target. The study is carried out under movable and dynamic conditions of biological systems promoting powerful interaction of the ligand with its target (Hollingsworth and Dror, 2018). Complex stability is evaluated with reference to Root Mean Square Deviation (RMSD) where a value of 1-3 Å is usually acceptable for small globular proteins. In the current study, MD simulation in water was conducted on S protein complexes of the top 8 ligands (Breeds 1-8) which were selected based on their high XP docking scores, good physiochemical characteristics and favorable binding free energies. RMSD values indicated that the ligand-protein complex for Breed 5 was the most stable and the ligand remained bound to protein binding pocket throughout the simulation that lasted for 50ns. Although the ligand–protein complexes for Breeds 3 and 6 were relatively more stable than the rest, small to high fluctuations were recorded in their RMSD plots (fig. 5).

Ligand interactions with the residues in ACE-2-RBD of S protein supported further the RMSD findings that Breed 5 was the best among the three molecules. During simulation, Breed 5 interacted with most of the residues in the target active site via hydrogen, ionic and hydrophobic bonds (fig. 6). The direct hydrogen bond and pi-cation interaction with TYR 505 remained stable during 75% and 57%, respectively, of all simulation time accounting, most probably, for the unique stability of Breed 5 when compared to 3 and 6. Moreover, GLY 496 also appeared to have a role in stabilizing the complex mediated by direct hydrogen bond and water bridges up to 24ns during simulation time. In addition, ASN 501 interacted with Breed 5 through relatively weaker water bridges which remained stable for nearly one third of the total time. Breed 3 complex with S protein displayed both hydrophilic and hydrophobic interactions during the process. Residues THR 500 and ASN 501 formed very stable hydrogen bonds and water bridges with Breed 3 accounting very much, with nearly equal contribution, for the complex stability. Furthermore, GLY 502 and GLN 498 helped stabilizing the complex for a short while as they bound Breed 3 via relatively weaker hydrogen bonds and water bridges. Very weak hydrogen bonds were observed in the interaction of Breed 3 with residues GLY

496, TYR 449, GLY 446 and VAL 503. The amino acid TYR-505 interacted with Breed 3 via hydrophobic bonding (fig. 6). The two major amino acids that bound Breed 6 were TYR 499 and GLY 496 through direct hydrogen bond and water bridges. In addition, TYR had hydrophobic interaction with Breed 6 (fig. 6).

HOMO-LUMO gap has a crucial role in stabilizing the interactions between a drug and its target protein (Zheng *et al*., 2013). The HOMO and LUMO distributions, energies, and energy gaps along with electrostatic potential maps of the top three breeds (3, 5 and 6) were calculated in the current study and reported herein (table 2; fig. 7).

The lowest excitation energy of a molecule is related to HOMO-LUMO energy gap which is directly proportional to the chemical stability and hardness of the molecule (Miar *et al*., 2021). In this study, frontier molecular orbitals (FMOs) calculation studies on Breeds 3, 5 and 6 revealed energy ranges of (-0.22373 to -0.23337 ev) and (-0.05720 to -0.07415 ev) for HOMO and LUMO, respectively. Moreover, HOMO-LUMO energy gap ranged from 0.15015 eV to 0. 0.17617 ev indicating potential chemical reactivity which would be useful for bioactivity-guided structural derivatization. In fig. 7, molecular electrostatic potential (MESP) maps indicate the accessible regions for electrophiles and nucleophiles by red and blue color, respectively. Taking into consideration that HOMO, being occupied by electrons, is the electron donor whereas the acceptor is LUMO, it is believed that both orbitals control the mode by which a drug binds its receptor. During the binding process, the drug's HOMO could share orbital interactions with the LUMO of adjacent residues (Hagar *et al*., 2020). Interestingly, Breed 5, the best ligand based on MD studies, interacted with some residues in S protein active site via hydrogen bonds involving three nitrogen atoms where HOMOs are located. The amino nitrogen atom (N10) exhibited hydrogen bonds with Tyr 505 and GLY 496. Hydrogen bonds were also observed for nitrogen atoms 1 and 6 with ARG 403 and GLY 496, respectively.

Exploration of Zinc and ChEMBL databases revealed that Breed 5, being the best ligand that showed good stability during simulation, is a novel compound and it did not match any of the screened drugs, bioactive molecules or commercially available compounds. Thus, addressing synthetic accessibility of Breed 5 is critical to validate, experimentally, the revealed activity (Ertl and Schuffenhauer, 2009). Reaction based enumeration Pathfinder has been a useful Schrodinger tool that retro-synthetically predicts pathways for synthesis of any compound. Breed 5 was subjected to retro-synthetic analysis using Pathfinder resulting in a variety of potential synthetic pathways. Fortunately, SwissSimilartity server demonstrated that synthesis of Breed 5 is feasible (synthetic accessibility score = 3.69) (Zoete, Daina *et al*., 2016).

CONCLUSION

A pharmacophore hypothesis was generated based on the amino acid residues in the receptor binding domain of SARS-COV-2 spike protein. Exploring three fragments' libraries revealed 80000 pharmacophore matching fragments which were virtually screened against spike protein. De novo synthesis of fragments exhibiting XP score ≤-6 kcal/mol resulted in 1848 ligand hybrids, 140 0f which had XP docking scores ≤-7 kcal/mol which were filtered further via molecular docking, MM-GBSA free energy calculation, ADMET, drug-like properties and DFT calculations. The study findings revealed 8 top ligand hybrids (Breeds 1-8) which were subjected to molecular dynamic simulation. The novel molecule Breed 5 formed the most stable interactions with the active site of spike protein. It is therefore reported, herein, as a new SARS-COV-2 host cell entry inhibitor lead which would be a good start towards COVID-19 drug discovery and development.

ACKNOWLEDGMENT

The authors are thankful to the Deanship of Scientific Research at Jouf University for funding this work under grant No.DSR-2021-01-03127. The authors acknowledge Mme Katia Dekimeche form Schrödinger for her technical support and help.

REFERENCES

Agrawal U, Katikireddi SV, McCowan C, Mulholland RH, Azcoaga-Lorenzo A, Amele S, Fagbamigbe AF, Vasileiou E, Grange Z and Shi T (2021). COVID-19 hospital admissions and deaths after BNT162b2 and ChAdOx1 nCoV-19 vaccinations in 2·57 million people in Scotland (EAVE II): A prospective cohort study. *Lancet Respir. Med.,* **9**(12): 1439-1449.

Ahsan T and Sajib AA (2021). Repurposing of approved drugs with potential to interact with SARS-CoV-2 receptor. *Biochem. Biophys. Rep.,* **26**: 100982.

Ameen F, Mamidala E, Davella R and Vallala S (2021). Rilpivirine inhibits SARS-CoV-2 protein targets: A potential multi-target drug. *J. Infect. Public Health,* **14**(10): 1454-1460.

Bassi LL. Hwenda L (2020). COVID-19: time to plan for prompt universal access to diagnostics and treatments. *Lancet Glob. Health*, **8**(6): e756-e757.

Bochevarov AD, Harder E, Hughes TF, Greenwood JR, Braden DA, Philipp DM, Rinaldo D, Halls MD, Zhang J and Friesner RA (2013). Jaguar: A high-performance quantum chemistry software program with strengths in life and materials sciences. *Int. J. Quantum Chem.,* **113**(18): 2110-2142.

Bowers KJ, Chow DE, Xu H, Dror RO, Eastwood MP, Gregersen BA, Klepeis JL, Kolossvary I, Moraes MA and Sacerdoti FD (2006). Scalable algorithms for molecular dynamics simulations on commodity clusters. SC'06: Proceedings of the 2006 ACM/IEEE Conference on Supercomputing, IEEE, p.43

Cecon E, Burridge M, Cao L, Carter L, Ravichandran R, Dam J and Jockers R (2021). SARS-COV-2 spike binding to ACE2 in living cells monitored by TR-FRET. *Cell Chem. Biol.,* **28**: 1-10

Choudhury C (2021). Fragment tailoring strategy to design novel chemical entities as potential binders of novel corona virus main protease. *J. Biomol. Struct. Dyn.,* **39**(10): 3733-3746.

Dixon SL, Smondyrev AM, Knoll EH, Rao SN, Shaw DE. Friesner RA (2006). PHASE: A new engine for pharmacophore perception, 3D QSAR model development and 3D database screening: 1. Methodology and preliminary results. *J. Comput. Aided Mol. Des.,* **20**(10): 647-671.

Elbadwi FA, Khairy EA, Alsamani FO, Mahadi MA, Abdalrahman SE, Ahmed ZAM, Elsayed I, Ibraheem W and Alzain AA (2021). Identification of novel transmembrane Protease Serine Type 2 drug candidates for COVID-19 using computational studies. *Inform. Med. Unlocked,* **26**: 100725.

Ertl P and Schuffenhauer A (2009). Estimation of synthetic accessibility score of drug-like molecules based on molecular complexity and fragment contributions. *J. Cheminform.,* **1**(1): 8.

Fadaka AO, Aruleba RT, Sibuyi NRS, Klein A, Madiehe AM and Meyer M (2020). Inhibitory potential of repurposed drugs against the SARS-CoV-2 main protease: A computational-aided approach. *J. Biomol. Struct.* Dyn., pp.1-13, doi.org/10.1080/07391102.2020. 1847197

Friesner RA, Murphy RB, Repasky MP, Frye LL, Greenwood JR, Halgren TA and Sanschagrin PC. Mainz DT (2006). Extra precision glide: Docking and scoring incorporating a model of hydrophobic enclosure for protein- ligand complexes. *J. Med. Chem.,* **49**(21): 6177-6196.

Giofrè SV, Napoli E, Iraci N, Speciale A, Cimino F, Muscarà C, Molonia MS, Ruberto G and Saija A (2021). Interaction of selected terpenoids with two SARS-CoV-2 key therapeutic targets: An in silico study through molecular docking and dynamics simulations. *Comput. Biol. Med.,* **134**: 104538.

Gobeil SM, Janowska K, McDowell S, Mansouri K, Parks R, Manne K, Stalls V, Kopp MF, Henderson R, Edwards RJ, Haynes BF and Acharya P (2021). D614G Mutation alters SARS-CoV-2 spike conformation and enhances protease cleavage at the S1/S2 junction. *Cell Rep.,* **34**(2): 108630.

Gupta P, Thomas SE, Zaidan SA, Pasillas MA, Cory-Wright J, Sebastián-Pérez V, Burgess A, Cattermole E, Meghir C, Abell C, Coyne AG, Jacobs WR, Jr., Blundell TL, Tiwari S and Mendes V (2021). A fragment-based approach to assess the ligandability of ArgB, ArgC, ArgD and ArgF in the L-arginine biosynthetic pathway of *Mycobacterium tuberculosis*. *Comput. Struct. Biotechnol. J.,* **19**: 3491-3506.

Hagar M, Ahmed HA, Aljohani G and Alhaddad OA (2020). Investigation of some antiviral N-heterocycles as COVID 19 drug: Molecular docking and DFT calculations. *Int. J. Mol. Sci.,* **21**(11): 3922.

Hollingsworth SA and Dror RO (2018). Molecular dynamics simulation for all. *Neuron.,* **99**(6): 1129-1143.

Jacobson MP, Pincus DL, Rapp CS, Day TJ, Honig B, Shaw DE and Friesner RA (2004). A hierarchical approach to all-atom protein loop prediction. *Proteins,* **55**(2): 351-367.

Kaur SP and Gupta V (2020). COVID-19 Vaccine: A comprehensive status report. *Virus Res.,* **288**: 198114.

Konze KD, Bos PH, Dahlgren MK, Leswing K, Tubert-Brohman I, Bortolato A, Robbason B, Abel R and Bhat S (2019). Reaction-based enumeration, active learning, and free energy calculations to rapidly explore synthetically tractable chemical space and optimize potency of cyclin-dependent kinase 2 inhibitors. *J. Chem. Inf. Model.,* **59**(9): 3782-3793.

Kyriakidis NC, Lopez-Cortés A, González EV, Grimaldos AB and Prado EO (2021). SARS-CoV-2 vaccines strategies: A comprehensive review of phase 3 candidates. *NPJ. Vaccines,* **6**(1): 28.

Lai CC, Shih TP, Ko WC, Tang HJ and Hsueh PR (2020). Severe acute respiratory syndrome coronavirus 2 (SARS-CoV-2) and coronavirus disease-2019 (COVID-19): The epidemic and the challenges. *Int. J. Antimicrob. Agents,* **55**(3): 105924.

Li Q (2020). Application of fragment-based drug discovery to versatile targets. *Front Mol. Biosci.,* **7**: 180.

Lopez Bernal J, Andrews N, Gower C, Gallagher E, Simmons R, Thelwall S, Stowe J, Tessier E, Groves N, Dabrera G, Myers R, Campbell CNJ, Amirthalingam G, Edmunds M, Zambon M, Brown KE, Hopkins S, Chand M and Ramsay M (2021). Effectiveness of Covid-19 vaccines against the B.1.617.2 (Delta) variant. *N. Engl. J. Med.,* **385**(7): 585-594.

Massinga Loembé M and Nkengasong JN (2021). COVID-19 vaccine access in Africa: Global distribution, vaccine platforms and challenges ahead. *Immunity,* **54**(7): 1353-1362.

Mesa-Vieira C, Botero-Rodríguez F, Padilla-Muñoz A, Franco OH. Gómez-Restrepo C (2021). The Dark Side of the Moon: Global challenges in the distribution of vaccines and implementation of vaccination plans against COVID-19. *Maturitas,* **149**: 37-39.

Meyers J, Fabian B and Brown N (2021). De novo molecular design and generative models. *Drug Discov. Today,* **26**(11): 2707-2715.

Miar M, Shiroudi A, Pourshamsian K, Oliaey AR. Hatamjafari F (2021). Theoretical investigations on the HOMO-LUMO gap and global reactivity descriptor studies, natural bond orbital, and nucleus-independent chemical shifts analyses of 3-phenylbenzo [d] thiazole-2 (3 H)-imine and its para-substituted derivatives: Solvent and substituent effects. *J. Chem. Res.,* **45**(1-2): 147-158.

Mohamed MA, Dirar AI, Elbadawi MA, Osman WJ, Mohammed MS and Hamdoun S (2017). *In silico* assessment of the druggability of two novel germacranolides isolated from Capparis decidua (Forsk.) as carbonic anhydrase II inhibitors. *J. App. Pharm. Sci.,* **7**(1): 093-097.

Munir MU, Salman S, Ahmed A, Iqbal W, Abbas Bukhari SN, Ahmad N, Ullah MI, Ahmad MM, Elsaman T and Tahir MA (2021). Covid-19: Diagnosis, summary of essays and evolving approaches. *Pak. J. Pharm. Sci.,* **34**(5): 1813-1820.

Ortega JT, Serrano ML, Pujol FH. Rangel HR (2020). Role of changes in SARS-CoV-2 spike protein in the interaction with the human ACE2 receptor: An in silico analysis. *Excli J.,* **19**: 410-417.

Rahman S, Montero MTV, Rowe K, Kirton R and Kunik F Jr (2021). Epidemiology, pathogenesis, clinical presentations, diagnosis and treatment of COVID-19: A review of current evidence. *Expert. Rev. Clin. Pharmacol.,* **14**(5): 601-621.

Sakkiah S, Guo W, Pan B, Ji Z, Yavas G, Azevedo M, Hawes J, Patterson TA and Hong H (2020). Elucidating interactions between SARS-CoV-2 trimeric spike protein and ACE2 using homology modeling and molecular dynamics simulations. *Front. Chem.,* **8**: 622632.

Santos LH, Ferreira RS and Caffarena ER (2019). Integrating molecular docking and molecular dynamics simulations., *Methods Mol. Biol.,* **2053**: 13-34.

Sastry GM, Adzhigirey M, Day T, Annabhimoju R and Sherman W (2013). Protein and ligand preparation: parameters, protocols and influence on virtual screening enrichments. *J. Comput. Aided Mol. Des.,* **27**(3): 221-234.

Tartof SY, Slezak JM, Fischer H, Hong V, Ackerson BK, Ranasinghe ON, Frankland TB, Ogun OA, Zamparo JM and Gray S (2021). Effectiveness of mRNA BNT162b2 COVID-19 vaccine up to 6 months in a large integrated health system in the USA: A retrospective cohort study. *The Lancet,* **398**(10309): 1407-1416.

Toor HG, Banerjee DI, Lipsa Rath S and Darji SA (2021). Computational drug re-purposing targeting the spike glycoprotein of SARS-CoV-2 as an effective strategy to neutralize COVID-19. *Eur. J. Pharmacol.,* **890**: 173720.

Walters WP and Murcko M (2020). Assessing the impact of generative AI on medicinal chemistry. *Nat. Biotechnol.,* **38**(2): 143-145.

Wilson III DM, Deacon AM, Duncton MA, Pellicena P, Georgiadis MM, Yeh AP, Arvai AS, Moiani D, Tainer JA and Das D (2021). Fragment-and structure-based drug discovery for developing therapeutic agents targeting the DNA damage response. *Prog. Biophys. Mol. Biol.,* **163**: 130-142.

Wollenhaupt J, Metz A, Barthel T, Lima GM, Heine A, Mueller U, Klebe G and Weiss MS (2020). F2X-universal and F2X-entry: Structurally diverse compound libraries for crystallographic fragment screening. *Structure,* **28**(6): 694-706. e695.

Yu R and Li P (2021). Screening of potential spike glycoprotein/ACE2 dual antagonists against COVID-19 in silico molecular docking. *J. Virol. Methods,* **301**: 114424.

Zeng MS, Yu WD, Wang HX, Liu JY and Xu PP (2021). A potential antiviral activity of Esculentoside A against binding interactions of SARS-COV-2 spike protein and angiotensin converting enzyme 2 (ACE2). *Int. J Biol. Macromol.,* **183**: 2248-2261.

Zhang Q, Gefter J, Sneddon WB, Mamonova T. Friedman PA (2021). ACE2 interaction with cytoplasmic PDZ protein enhances SARS-CoV-2 invasion. Iscience, **24**(7): 102770.

Zheng Y, Zheng M, Ling X, Liu Y, Xue Y, An L, Gu N and Jin M (2013). Design, synthesis, quantum chemical studies and biological activity evaluation of pyrazole-benzimidazole derivatives as potent Aurora A/B kinase inhibitors. *Bioorg. Med. Chem. Lett.,* **23**(12): 3523-3530.

Zoete V, Daina A, Bovigny C and Michielin O (2016). SwissSimilarity: A web tool for low to ultra high throughput ligand-based virtual screening. *J. Chem. Inf. Model.,* **56**(8): 1399-1404.